

Nanoscale

Accepted Manuscript



This is an *Accepted Manuscript*, which has been through the Royal Society of Chemistry peer review process and has been accepted for publication.

Accepted Manuscripts are published online shortly after acceptance, before technical editing, formatting and proof reading. Using this free service, authors can make their results available to the community, in citable form, before we publish the edited article. We will replace this *Accepted Manuscript* with the edited and formatted *Advance Article* as soon as it is available.

You can find more information about *Accepted Manuscripts* in the [Information for Authors](#).

Please note that technical editing may introduce minor changes to the text and/or graphics, which may alter content. The journal's standard [Terms & Conditions](#) and the [Ethical guidelines](#) still apply. In no event shall the Royal Society of Chemistry be held responsible for any errors or omissions in this *Accepted Manuscript* or any consequences arising from the use of any information it contains.

Antisense precision polymer micelles require less poly(ethylenimine) for efficient gene knockdown

Johans J. Fakhoury, Thomas W. Edwardson, Justin W. Conway, Tuan Trinh, Farhad Khan,

*Maciej Barłóg, Hassan S. Bazzi² and Hanadi F. Sleiman*¹*

1. Department of Chemistry and Center for Self-Assembled Chemical Structures, McGill University, 801 Sherbrooke St. W., Montreal, Quebec H3A 0B8 (Canada); 2. Department of Chemistry, Texas A&M University at Qatar, P.O. Box 23874, Doha, Qatar.

DNA, Sequence Polymer Antisense Delivery, Gene Silencing, DNA-polymer micelles.

Abstract

Therapeutic nucleic acids are powerful molecules for shutting down protein expression. However, their cellular uptake is poor and requires transport vectors, such as cationic polymers. Of these, poly(ethylenimine) (PEI) has been shown to be an efficient vehicle for nucleic acid transport into cells. However, cytotoxicity has been a major hurdle in the development of PEI-DNA complexes as clinically viable therapeutics. We have synthesized antisense-polymer conjugates, where the polymeric block is completely monodisperse and sequence-controlled. Depending on the polymer sequence, these can self-assemble to produce micelles of very low polydispersity. The introduction of linear poly(ethylenimine) to

these micelles leads to aggregation into size-defined PEI-mediated superstructures. Subsequently, both cellular uptake and gene silencing are greatly enhanced over extended periods compared to antisense alone, while at the same time cellular cytotoxicity remains very low. In contrast, gene silencing is not enhanced with antisense polymer conjugates that are not able to self-assemble into micelles. Thus, using antisense precision micelles, we are able to achieve significant transfection and knockdown with minimal cytotoxicity at much lower concentrations of linear PEI than previously reported. Consequently, a conceptual solution to the problem of antisense or siRNA delivery is to self-assemble these molecules into ‘gene-like’ micelles with high local charge and increased stability, thus reducing the amount of transfection agent needed for effective gene silencing.

Introduction

Nucleic acid delivery for therapeutic purposes has been, and is still, a very promising method for treating different diseases that are otherwise untreatable with conventional small-molecule therapeutics. Taking advantage of the RNase H degradation pathway and innate RNAi mechanisms transforms “undruggable” diseases into “druggable” and controllable alternatives. However, the success of these approaches has been dependent on the development of highly efficient nucleic acid carriers. Exploiting the tropisms and characteristics of viruses is one approach for enhanced nucleic acid delivery. This approach, though highly promising, has been marred by problems with immunogenicity¹ and high cost.² Alternatively, non-viral carriers seek to mimic viral capsid efficiency by artificial means while being easily synthesized and inducing low immunogenicity.³ Almost universally, most of these synthetic strategies are cationic polymers or lipids which form self-assembled polyelectrolyte complexes with nucleic acids, facilitating cellular uptake and endolysosomal escape.⁴

To date, many cationic compounds have been developed as carriers. However, ethylenimine polymers (poly(ethylenimines), PEIs), remain the gold-standard for the development of new gene carriers. The first report demonstrating the prominent transfection efficiency of PEI was published in 1995.⁵ Since then, many reports have confirmed these observations and further explored the mechanism of PEI-mediated-nucleic acid uptake. PEIs interact directly with DNA through their positively charged amino groups thus condensing DNA into complexes with an overall positive charge. Subsequently, cationic PEI/nucleic acid particles interact with anionic proteoglycans on the cell surface^{6,7} and are internalized via at least two different endosomal pathways, the clathrin- and the caveolae/raft-dependent routes.⁸ Endosomal escape is often attributed as the leading mechanism for the high transfection efficiency of PEI. In endosomal compartments, PEI is able to buffer the pH causing a large build-up of ionic concentration, which results in osmotic swelling. Additionally, internal charge repulsion leads to polymer expansion.⁵ Ultimately, this will cause destabilization and rupturing of endosomal membranes leading to the release of PEI/DNA complexes into the cytosol. This has been termed the “proton sponge effect”.⁹ As the complexes transition through the cytosol, it was demonstrated that PEI:DNA complexes are initially protected from degradation¹⁰ but DNA can undergo decondensation from PEI in the cytosol¹¹ potentially allowing antisense nucleic acid molecules to exert their therapeutic effect.

Unfortunately, highly efficient DNA (plasmid DNA) carriers such as branched (B-PEI) and linear PEI (L-PEI), form poor carriers of antisense oligonucleotides¹² and siRNA molecules.¹³ Grayson and colleagues demonstrated that only B-PEI induced specific RNA interference at high concentrations at which cytotoxicity becomes a noticeable concern.¹³ It has been suggested that the lower number of anionic charges present (in siRNA duplexes and antisense strands compared to plasmid DNA) reduces the electrostatic cohesion between PEI and these nucleic acid molecules, resulting in reduced cooperative binding.¹⁴ The use of lower molecular weight PEI greatly reduces cytotoxicity. However, this comes at the cost of poor transfection efficiency.¹⁵⁻¹⁷ In order to overcome this limitation, PEI chemistry can be altered by conjugation to lipidic moieties, leading to enhanced delivery of short nucleic acids.^{12, 18} Other

approaches to reduce cytotoxicity involve cyclizing LMW PEIs.¹⁹ A recent report demonstrated that introduction of PEI to biodegradable nanoparticles enhanced transfection efficiency and gene silencing.²⁰ Interestingly, enhanced gene silencing was observed when siRNA with sticky overhangs were used with PEI. These siRNA strands oligomerized to form ‘gene-like’ particles that bound more strongly to PEI.²¹ Thus, creating nucleic acid particles that resemble highly negatively charged plasmids can be a promising avenue for PEI-mediated gene silencing.

We recently reported the facile and high yielding synthesis of a new class of DNA-polymer conjugates via automated solid-phase synthesis.²² Unlike most synthetic macromolecules, the polymers attached to DNA are fully monodisperse and sequence-controlled. These DNA-polymer conjugates (**DPs**) can incorporate long chain aliphatic, aromatic, metal coordinating, polyfluorinated and oligo(ethylene glycol) units with control over the sequence of monomers. By introduction of dodecane diol polymer blocks with hydrophobic character DNA-amphiphiles can be created, which spontaneously self-assemble into highly monodisperse spherical micelles in solution.²² Several examples in recent years have emerged demonstrating the suitability of DNA nanostructures for nucleic acid delivery such as spherical nucleic acid particles, among others.²³⁻²⁸ Often these self-assembled DNA structures require many unique strands to produce the effective target structure,^{29, 30} raising issues of scalability and immunogenicity/off-target effects. **DP** micelles have the advantage of producing well-defined, monodisperse nanoparticles while only using a single DNA/RNA sequence and a polymer modification. The resulting DNA-polymer micelles are capable of encapsulating small molecule drugs in their core while retaining the molecular recognition properties of DNA.²² DNA-based micelles have been shown previously to have enhanced cellular uptake profiles,³¹⁻³³ and are therefore a potentially useful delivery strategy for nucleic acid therapeutics. Furthermore, DNA-polymer micelles have been shown to effect gene silencing by conjugating locked nucleic acid-stabilized oligonucleotides directly to hydrophobic polymers.³⁴ In the present study, we have synthesized micelle-forming antisense (ASO)-polymer conjugates and condensed them with L-PEI in order to achieve high transfection efficiency with minimal cytotoxicity.

Under these conditions, unmodified antisense oligonucleotides do not effect gene knockdown. Moreover, we demonstrate that gene silencing is dependent on the ability of the monomeric sequence to form a micellar structure that greatly enhances degradation resistance and gene silencing. Using an ASO polymer conjugate with a different monomer sequence, that is incapable of forming micelles does not result in PEI-mediated gene silencing. Thus, a conceptual solution to the problem of antisense or siRNA delivery is to self-assemble these molecules into 'gene-like' micelles with high local charge and increased stability, thus reducing the amount of transfection agent needed.

Experimental Section

Materials

Magnesium acetate, acetic acid, tris(hydroxymethyl)-aminomethane (Tris), formamide, and urea were used as purchased from Sigma-Aldrich. Acetic acid and boric acid were purchased from Fisher Scientific and used without further purification. GelRed™ nucleic acid stain was purchased from Biotium Inc. Acetone ACS reagent grade was purchased from Fisher. Ammonium citrate dibasic and 3-hydroxypicolinic acid were purchased from Aldrich. Acrylamide/Bis-acrylamide (40% 19:1 solution) and TEMED were obtained from Bioshop Canada Inc. and used as supplied. 1 mol Universal 1000Å LCAACPG supports and standard reagents used for automated DNA synthesis reagents were purchased through Bioautomation. Sephadex G-25 (super fine, DNA grade) was purchased from Glen Research. TAMg buffer is composed of 45 mM Tris and 12.5 mM Mg(OAc)₂·6H₂O with pH adjusted to 8.0 using glacial acetic acid. TBE buffer is 90mM Tris, 90mM boric acid and 1.1mM EDTA with a pH of 8.0. L-PEI 25 kDa, 2.5 kDa, and B-PEI 1.8 kDa were purchased from Polysciences Inc. (USA). L-PEI 5 kDa was purchased from Sigma-Aldrich (USA).

Synthesis and Characterization of ASO-polymer conjugates

The DNA synthesis was based on previous work by Edwardson et al.,²² using universal 1000 Å CPG solid-supports (BioAutomation, cat.# MM1-3500-1). Cy3 phosphoramidite (cat.# 10-5913) was

purchased from Glen Research. DMT-dodecane-diol (cat.# CLP-1114) and DMT-hexaethoxy glycol (cat.# CLP-9765) phosphoramidite were purchased from ChemGenes. All non-standard amidites were dissolved to 0.07 M in anhydrous acetonitrile, with extended coupling times of 5 minutes. Coupling efficiency was monitored after removal of the dimethoxytrityl (DMT) 5'-OH protecting groups, using 3% DCA in dichloromethane. Completed syntheses were deprotected in 1 mL of 1:1 v/v mixture of 40% aqueous Methylamine and 28% aqueous ammonium hydroxide solution for 3 hours at 65°C. The crude deprotected solution was separated from the solid support and concentrated under reduced pressure at 60°C. This crude solid was re-suspended in 0.2 mL sterile water in preparation for purification by reverse-phase HPLC.

Atomic Force Microscopy

All images were obtained using tapping mode in air with Tap300Al-G cantilevers (Nominal values: Tip radius - <10nm, Resonant frequency – 300kHz, Force constant – 40 N/m) from Asylum Research. Samples were diluted to 1-4 μ M in 1xTAMg buffer and 5 μ L of this solution was deposited on a freshly cleaved mica surface (ca. 7 x 7 mm) and allowed to adsorb for 1-2 seconds. Next, 50 μ L of 0.22 μ m filtered Millipore water was dropped on the surface and instantly removed with filter paper. The surface was then washed with a further 4x50 μ L of water and the excess removed with a strong flow of nitrogen. Samples were dried under vacuum for 10-20 minutes prior to imaging.

Transmission Electron Microscopy

TEM samples were simply prepared by depositing 3 μ L of sample solution (1 μ M, 1xTAMg) onto the carbon-coated grid. After 90 seconds, the droplet was removed using filter paper and the grid was held under vacuum for 4 hours before microscopy.

Zeta potential Analysis

DNA-conjugates were annealed into micelles, and subsequently incubated with PEI to a concentration of 3.6 μ M and volume of 500 μ L in 1X Tris-Magnesium-Acetate buffer, pH 8.0. The sample was then diluted to 700 μ L upon measurement of the zeta potential (ζ), at 25° C on a Zetasizer Nano ZS (Malvern Instruments, Malvern, UK). The zeta potential was calculated from the electrophoretic mobility as per the Smoluchowski approximation. The values are presented are an average of 30 runs across four measurements per replicate.

Dynamic Light Scattering

Samples, water and buffer were filtered using a 0.22 μ m nylon syringe filter prior to use in DLS sample preparation. Scattering measurements were carried out at 25 °C, and a cumulants fit model was used to determine the size and distribution of spherical particles. For the PEI-ASO complexes the PEI and oligonucleotide solutions were mixed and incubated at room temperature for 10 minutes prior to measurement.

Cell Culture

HeLa cells were maintained in 10% FBS and antibiotic/antimycotic (AB/AM) and cultured in 5% CO₂ at 37°C. Typically, cells were split in 1:4 ratio every 3 days.

Cytotoxicity Assay

The cytotoxicity of the different PEIs was assessed using the CellTiter Blue kit from Promega according to the manufacturer's instructions. Briefly, HeLa cells (human cervical cancer) were seeded at a density of 5000 cells per well in a 96-well plate in DMEM media (Invitrogen) supplemented with 10% FBS and AB/AM. Stock solutions of PEI salt complexes (1 μ g/1 μ L) were initially diluted in DEPC (Diethylpyrocarbonate)-treated water. Final concentrations of PEI were varied and maintained according to different N:P ratios. Cells were incubated for 24 h in 5% CO₂ at 37°C. After the incubation period, the fluorescent reagent (CellTiter Blue) was added to each well and further incubated for 3 h in 5% CO₂ at

37°C. Subsequently, 96-well plates were allowed to equilibrate at room temperature and the fluorescence was measured at 590 nm (Ex. 530, Em. 590) using a BioTek Synergy HT micro-plate reader. All quantifications were done using GraphPad Prism 5 software.

Luciferase Knockdown Assay

Luciferase knockdown assays were performed as described in Deleavey et al.³⁵ with a few modifications. Typically, HeLa cells were counted and seeded at a density of 10,000 cells/well in a 96-well plate. Cells were allowed to recover for 24, 48, and 72 hours at 37°C with 5% CO₂. Subsequently, cells were washed once with serum-free DMEM (Dulbecco's modified eagle medium) media and then 80 µL of serum-free DMEM media was added. DNA-polymer conjugates and control PEI preparations (80 nM final concentration) were diluted up to 20 µL with serum-free media and transfection reagent (N:P 1, 2, 4, 8, 10) and added to the appropriate well (for a total of 100 µL). Lipofectamine reagent was used as transfection control (Invitrogen). Cells were supplemented with 50 µL of serum-enriched DMEM media. Cells were further incubated overnight (for a total of 24 hours post-DNA addition). Then cells were washed with PBS 1X and lysed with Glo-lysis buffer (Promega). Subsequently, 100 µL of Bright-Glo luciferase reagent (Promega, USA) was added to each well and luminescence Biotek Synergy HT plate reader. Data was acquired with the Gen5 software suite and data was manipulated and plotted using Graphpad Prism software suite.

Fluorescence Microscopy

Fluorescence cell imaging was performed with a Zeiss Axio Imager. Typically, HeLa cells were counted and seeded at a density of 50,000 cells/well in an 8-well slide. Cells were allowed to recover for 24 hours at 37°C with 5% CO₂. Subsequently, cells were washed once with serum-free DMEM media and then 350 µL of DMEM media was added. DNA-polymer conjugates and control nucleic acid preparations (100 nM final concentration) were diluted up to 50 µL with serum-free media and added to the appropriate well. Cells were then washed 3 times with phosphate-buffered saline (PBS) and fixed in with a 4% paraformaldehyde/PBS solution. Cells were further washed thrice with PBS. Fixed cells were then

mounted with Prolong Gold®(Invitrogen) and visualized after curing overnight at 4°C. All images were acquired and manipulated using Zen (Zeiss) software suite.

Endocytosis inhibition

HeLa cells were seeded in a 96-well plate at a density of 5×10^3 cells/well. After 24 h of incubation at 37°C, cells were washed and then treated with media containing wortmannin (10 μ M), filipin (1 μ M), or sucrose (0.45 M) for 1 h or 24 hours. Wortmannin, filipin, and sucrose are specific inhibitors of macropinocytosis, caveolae/lipid raft-mediated endocytosis, and clathrin-mediated endocytosis respectively. After removing growth media with inhibitors, cells were treated with antisense/polymer/PEI mixes and luciferase levels were detected as described earlier.

Results and Discussion

DNA-Polymer Conjugates

For this study, we used three different DNA constructs. First, a phosphorothioate antisense oligonucleotide (ASO) against firefly luciferase was used as control. The second structure is the same ASO, conjugated to a sequence and length-controlled polymer, with twelve dodecane units (**HE₁₂-Luc-ASO**, Fig.1). The third is the ASO conjugated to a polymer with an alternating sequence of hexaethylene glycol and dodecane units (**(HE-HEG)₆-Luc-ASO**, Fig. 1). Based on our previous report of DNA polymer micelles,²² the phosphorothioate DNA-polymer conjugate **HE₁₂-Luc-ASO** is expected to form spherical micelles in aqueous media containing divalent cations. A simple thermal annealing of **HE₁₂-Luc-ASO** provides micelles with low polydispersity (95-4°C, 1 hour, [Zarudnaya, #1107] = 4 μ M, TAMg buffer). The resulting solutions were studied using dynamic light scattering (DLS), atomic force microscopy (AFM) and transmission electron microscopy (TEM) to confirm micelle formation, Fig. 2. The data from each technique corroborated the formation of a monodisperse population of spherical micelles with a hydrodynamic radius of 8.6 nm. In contrast **(HE-HEG)₆-Luc-ASO** did not assemble into

any distinct structures, in accordance with the alternating distribution of hydrophilic and hydrophobic units on the polymer backbone.²²

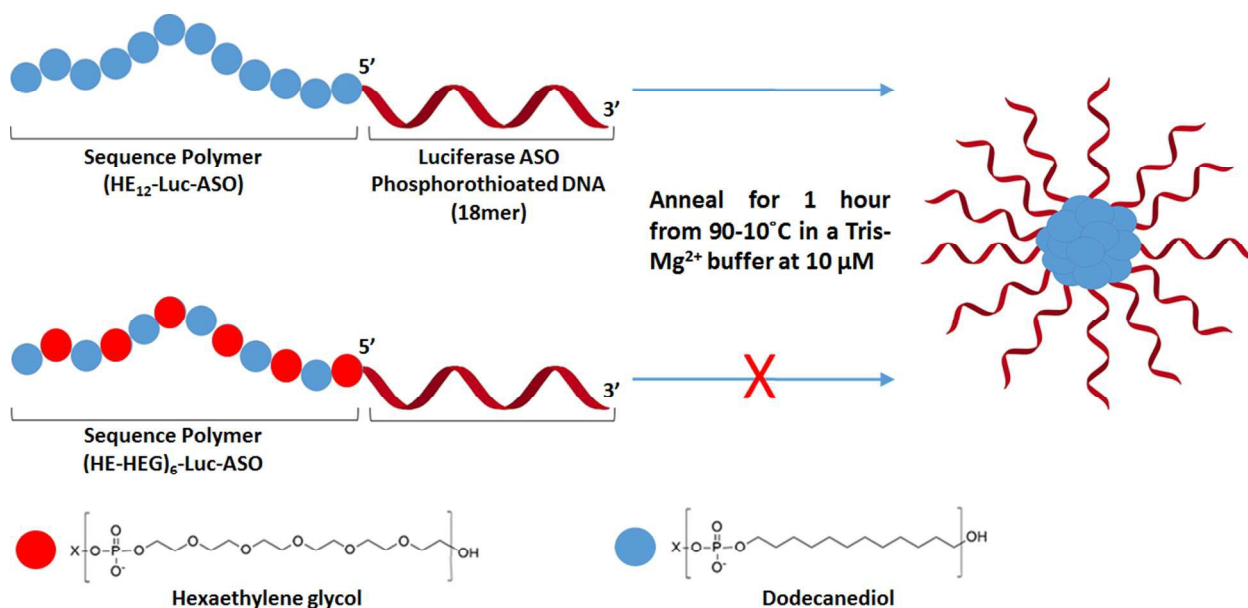


Figure 1 - Precision polymers conjugated to antisense oligonucleotides (ASO). (Top) ASO polymer with 12 dodecane (C12) repeat units self-assembles into micelles in aqueous media. (Bottom) ASO polymer with an alternating sequence of hexaethylene glycol-dodecane units does not assemble into micelles in aqueous media.

With the size and structure of the **HE₁₂-Luc-ASO** micelles determined we were next interested in studying the **HE₁₂-Luc-ASO:PEI** complexes. Here we focus on the 25kDa L-PEI at an N:P ratio of 10, as this gave the most promising results in the in vitro gene silencing experiments (detailed below). As the mechanism of uptake is unknown, an investigation into the presence of any stable structure may provide clues into the effectiveness of the micelle:polycation platform. In each case **HE₁₂-Luc-ASO** micelles were prepared as described and 25kDa L-PEI (in TAMg buffer) was added to produce the N:P=10

complexes at $4\mu\text{M}$ of DNA. After a 10 minute incubation period, the samples were analyzed. As can be seen in Fig. 2B, a large jump in hydrodynamic radius from $8.6 \pm 0.1\text{ nm}$ to $41.3 \pm 2.6\text{ nm}$ is seen, suggesting aggregation of the **HE**₁₂-**Luc**-**ASO** micelles into a larger superstructure by PEI. Figure 2A represents this structure as an aggregate of micelles, however, presently we are investigating whether the micelles are intact within this aggregate. Additionally, AFM and TEM showed the presence of large globular structures, with radii of $42.8 \pm 9.1\text{ nm}$ and $54.7 \pm 16.3\text{ nm}$ respectively. The narrow polydispersity for these polyelectrolyte complexes may be due in part to the monodisperse **HE**₁₂-**Luc**-**ASO** micelles. Zeta potential measurements showed negative values for the ASO strand and the ASO micelle, which increased to values close to $+60\text{ mV}$ upon PEI complexation. (Fig. SF12)

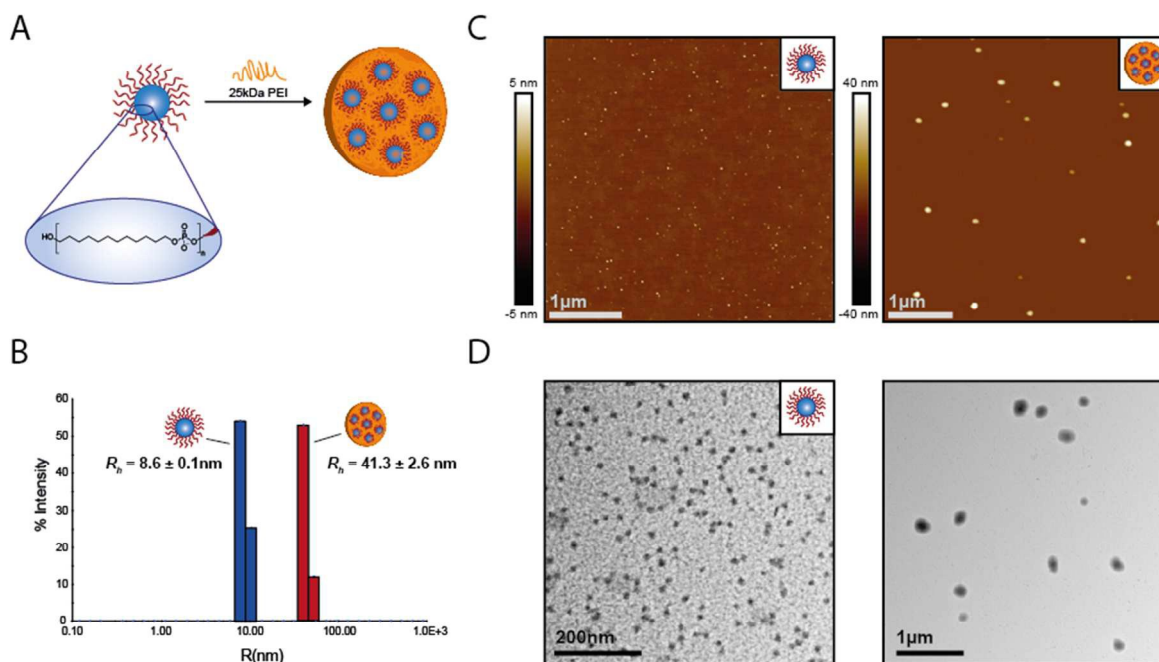


Figure 2 – Structural characterization of ASO/PEI complexes. a) Scheme for PEI-mediated aggregation of **HE**₁₂-**Luc**-**ASO** micelles. The resulting product is shown as an aggregate of micelles for illustrative purposes only. b) Dynamic light scattering data, showing an increase in hydrodynamic radius upon addition of 25kDa PEI to **HE**₁₂-**Luc**-**ASO** micelles. c) Atomic force microscopy of **HE**₁₂-**Luc**-**ASO** micelles (left panel) and **HE**₁₂-**Luc**-**ASO**:**PEI** complexes (right panel). D) Transmission electron

microscopy images of **HE₁₂-Luc-ASO** micelles (left panel) and **HE₁₂-Luc-ASO:PEI** complexes (right panel). All **HE₁₂-Luc-ASO:PEI** complexes here were assembled at 4 μ M with an N:P ratio of 10.

In Vitro Cytotoxicity

When considering PEI for non-viral nucleic acid delivery, a balance has to be struck between high transfection efficiency and low threshold cytotoxicity. Low MW (LMW) PEIs are known to be poor vectors compared to high MW (HMW) PEIs (>20 kDa) while being less cytotoxic. In our approach we first wanted to choose an appropriately sized PEI polymer to achieve this delicate balance. To this end, we tested four different polymers (Fig. 3) for in vitro cytotoxicity in HeLa cells using the CellTiterBlue Assay (Promega) (Fig. 3A). In the panel of PEIs we included a LMW Linear-PEI (2.5 kDa), an intermediate PEI (5 kDa) and a High MW (HMW) PEI (25 kDa). In addition we tested a LMW Branched-PEI (B-PEI). As indicated in Fig. 3A, cell cytotoxicity after 24 hours incubation was minimal when L-PEI were incubated with cells, even at higher concentrations of L-PEI (20 μ g/mL), however, B-PEI induced significant cytotoxicity, observed at very low concentrations of PEI (0.8 μ g/mL). We then proceeded with L-PEI 25 kDa as the preferred PEI to complex with our DNA-polymer conjugates, as the LMW L-PEIs are known to be inefficient nucleic acid carriers while B-PEIs tend to be significantly toxic.^{36, 37} We did also test gene silencing with LMW L-PEI (2.5 and 5 kDa), but we did not observe any knockdown (Fig. SF13).

Next, we tested the in vitro cytotoxicity of DNA-polymers and DNA (antisense oligonucleotide) when associated with L-PEI (25 kDa) (Fig. 3B). We observed minimal cytotoxicity at nitrogen to phosphate (N:P) ratios of 1, 10, and 30 for all complexes (0.067-4.8 μ g/mL) (Fig. 3B). In short, L-PEI (25 kDa) exhibited minimal cytotoxicity in HeLa cells at the concentrations of PEI employed (N:P=30 or 4.8 μ g/mL). However, it is known in the literature that further increase of PEI concentration (> 10 μ g/mL) leads to a significant increase in cytotoxicity.

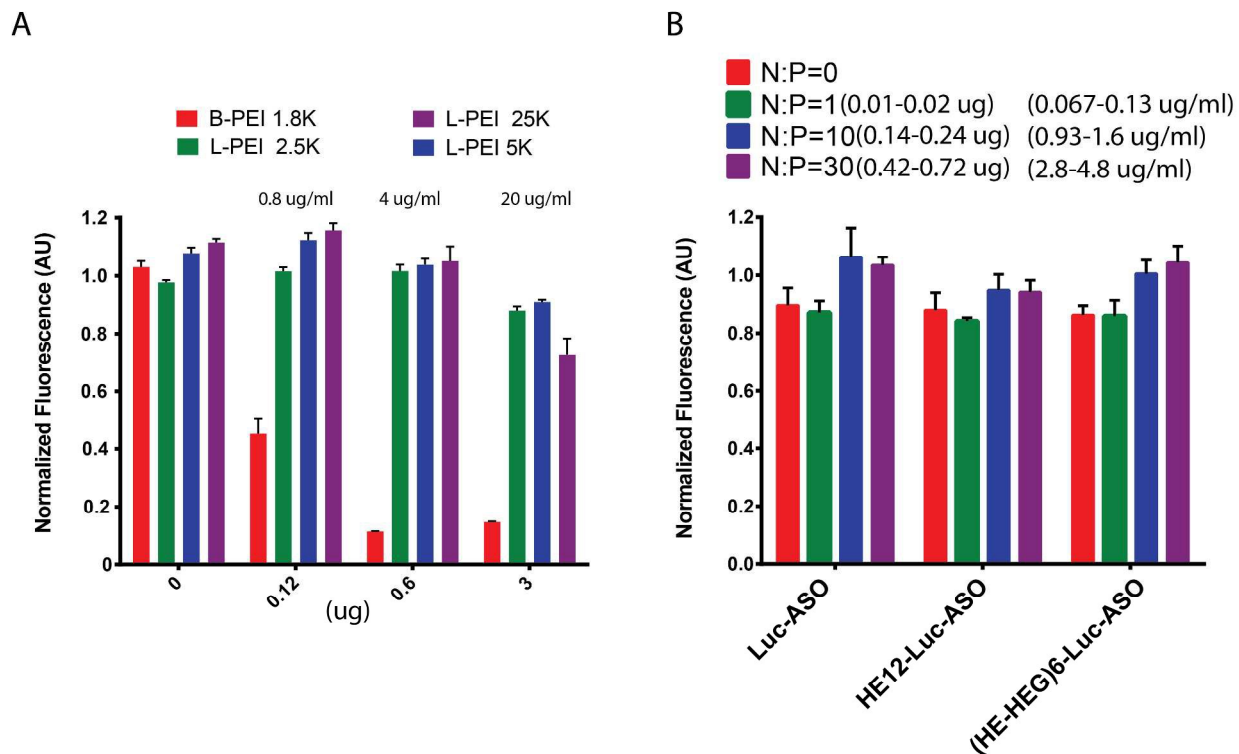


Figure 3. In vitro cytotoxicity of PEI and PEI-DNA-Polymers. A) Cytotoxicity of PEI alone was assessed in HeLa cells over 24 hours. Cells were incubated with increasing concentrations of linear PEI and branched PEI (0.8 $\mu\text{g/ml}$ -20 $\mu\text{g/ml}$). Fluorescence was normalized over untreated samples. B) Cytotoxicity of PEI- DP micelles was measured after 24 hours of incubation. Fluorescence was normalized to PEI only-treated samples.

Firefly Luciferase Knockdown Activity of ASO-Polymer/PEI Complexes

Previous work has shown that when L-PEI is used at greater than 10 $\mu\text{g/mL}$, significant cytotoxicity is incurred.³⁸ If L-PEIs are used at lower N:P ratios in order to minimize cytotoxicity, their potential for nucleic acid delivery is significantly reduced.³⁹ Alternatively, B-PEI could be used for effective ASO delivery, but only at N:P > than 10 and with concomitant cytotoxicity.³⁹ Thus, we were interested to study the knockdown potential of antisense oligonucleotide alone and when conjugated to micelle-forming (**HE**₁₂-Luc-ASO) and micelle-incapable ((**HE-HEG**)₆-Luc-ASO) below the cytotoxicity threshold (N:P \leq 30 and 4.8 $\mu\text{g/mL}$) (Fig. 4). This was carried out over 24, 48, and 72 hours in HeLa cells

expressing Firefly Luciferase (described earlier). Samples were prepared at 10 μ M and PEI was added to achieve an N:P ratio of 10 and a final concentration of 80 nM. We observed that under typical culture conditions (10% FBS) both **Luc-ASO** and **HE₁₂-Luc-ASO** achieved little gene silencing (Fig. 4A). However, after incubating for 48 and 72 hours, HE12-Luc-ASO achieved significantly increased gene silencing compared to Luc-ASO alone. Additionally, when the content of FBS was increased to 30%, enhanced gene silencing for **HE₁₂-Luc-ASO** relative to **Luc-ASO** alone was even more significant over 24, 48, and 72 hours (Fig. 4B). Interestingly, we observed enhanced activity of **HE₁₂-Luc-ASO** compared to antisense alone at a lower N:P=5 (Fig. SF8-A). On the other hand, non-micelle-forming polymers (**HE-HEG**)₆-**Luc-ASO** failed to achieve any appreciable knockdown at N:P=10 and was significantly less effective than HE12-Luc-ASO at higher N:P (Fig. SF9). In order to ascertain the knockdown functionality of ASO and ASO-polymers (**HE₁₂-Luc-ASO**), we validated knockdown with a commercially available transfection reagent (Lipofectamine, Fig. SF10). At 24 hours, Luc-ASO was significantly more potent than **HE₁₂-Luc-ASO**, however, after an extended period of incubation (72 hours), **HE₁₂-Luc-ASO** exhibited enhanced gene silencing compared to **Luc-ASO** alone.

We were further interested in investigating whether gene silencing persists after the removal of the initial DNA-PEI mixture. As described earlier we added each of **Luc-ASO** and **HE₁₂-Luc-ASO** and complexed with PEI N:P=10; however, we removed the media containing the mixture after 24 hours, replaced it with fresh media, and incubated the cells for 5 more days (Fig. 4C). We observed that **Luc-ASO** was completely inactive after this period. Surprisingly, **HE₁₂-Luc-ASO** remained significantly active after 120 hours under moderate (10% FBS) and increased (30% FBS) levels of fetal bovine serum content.

Here we show that at moderately low N:P ratios, antisense conjugated to micelle-forming polymers in the presence of low levels of L-PEI (<20 μ g/mL), is significantly more efficient at gene silencing compared to antisense alone with minimal cytotoxicity even after extended periods of incubation. The fact that enhanced gene silencing is more pronounced at longer incubation times and at higher FBS content, suggests that resistance to degradation could be an important factor contributing to this effect.

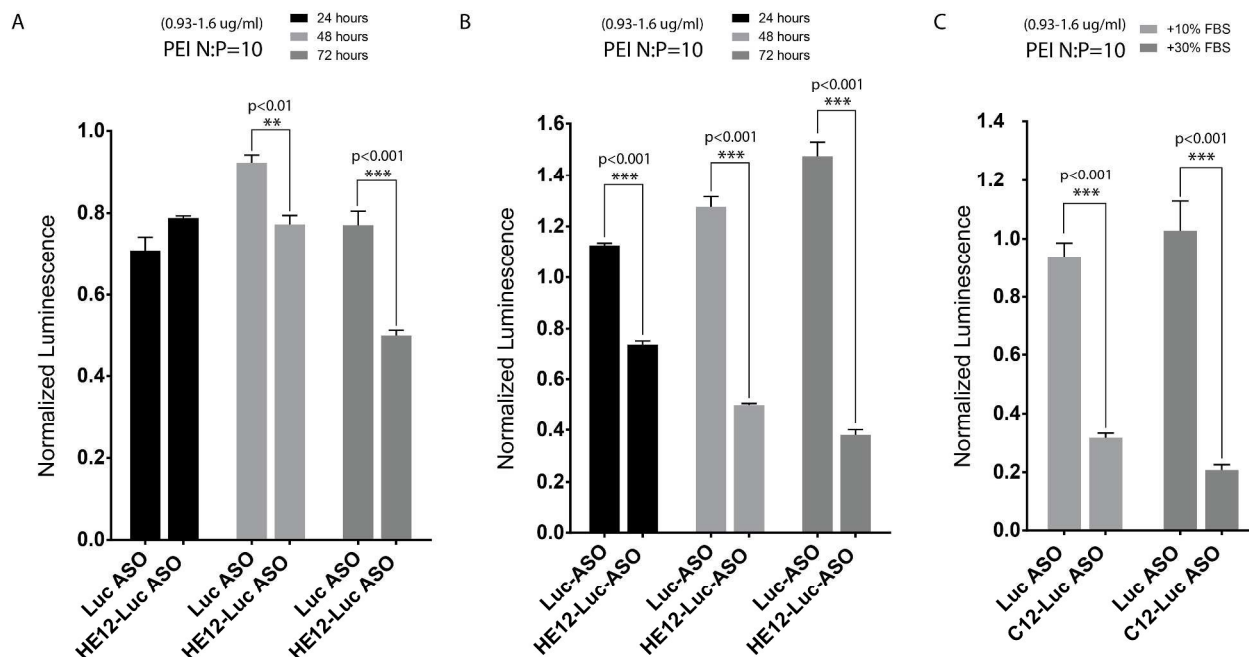


Figure 4 - Firefly Luciferase Knockdown Activity of ASO-Polymer/PEI Complexes. Firefly luciferase activity was measured after treatment with ASO alone and ASO-polymer complexes. Samples were incubated for 24, 48, and 72 hours at a ratio of N:P=10 with a final concentration of 80 nM in the presence of (A) 10% FBS and (B) 30% FBS. (C) DNA samples in the presence of PEI N:P=10 were incubated for 24 hours and subsequently replaced with fresh media. Cell were further incubated for 120 hours.

Cellular Localization of DNA-polymers in the presence of PEI

Previous studies have shown that uptake of PEI-complexed structures is largely dependent on the endocytic pathway and DNA-polymers in the presence of PEI are mostly localized to the cytoplasm.¹² Additionally, uptake efficiency of PEI-complexes increases with increasing N:P ratios.³⁶ Thus we proceeded to track the localization of **DP** micelles in the presence of PEI in HeLa cells (Fig. 5). In the presence of PEI, **DP** micelles are mostly found in the cytoplasm in perinuclear region which is indicative of endocytic uptake (Fig. 5A). Several intense foci are observed, confirming the high efficiency of uptake. In contrast, when LipofectamineTM (a commercial cationic transfection reagent) was used with the same

concentration of **DP** micelles (100 nM) for transfection, minimal uptake was observed (Fig. 5B). We were only able to observe foci of **DP** micelles in the presence of Lipofectamine when we overexposed the image (10 ms vs 370 ms - Fig. 5C).

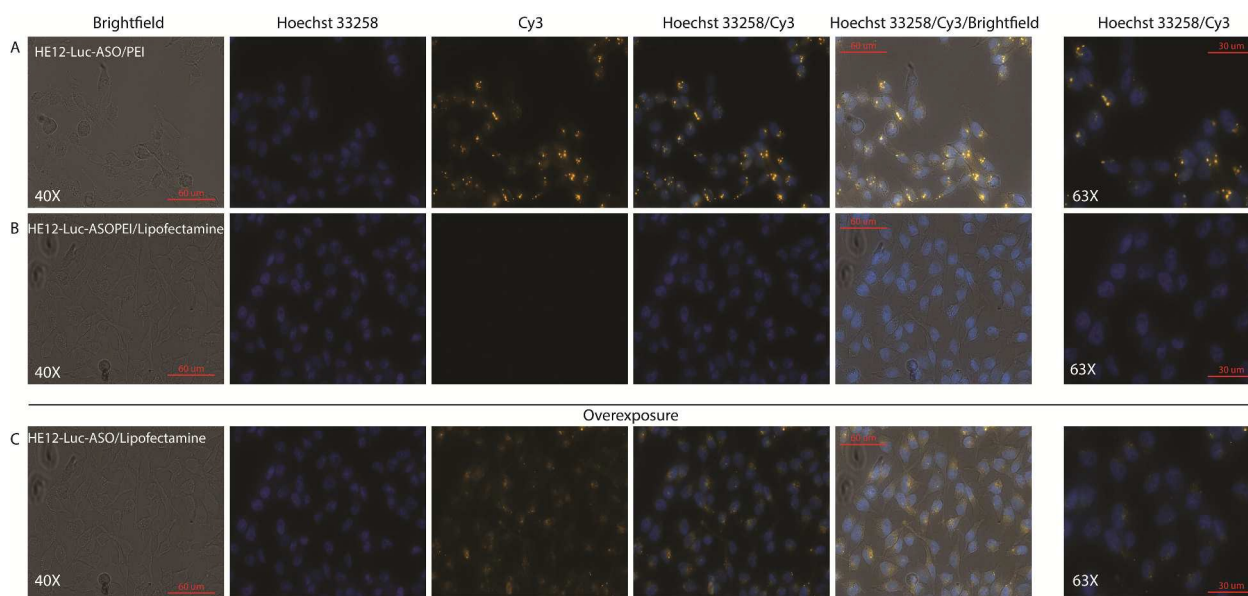


Figure 5 - Cellular Localization of DNA-Polymer/PEI Complexes. Fluorescence microscopy of PEI and Lipofectamine complexes was performed at N:P=10. All samples were incubated over night for 24 hours. DNA-polymer complexes were viewed in the Cy3 channel and Hoechst 33258 was used as a nuclear counterstain. Images were taken at 40X and 63X magnifications. (C) Represents the same images of DNA-polymer/Lipofectamine where the exposure in the Cy3 channel was increased (17 vs 370 milliseconds).

In order to ascertain that mechanism of uptake is indeed through endocytosis, we proceeded to test knockdown before and after the treatment with inhibitors targeting specific pathways of endocytosis. Wortmannin, filipin, and sucrose are specific inhibitors of macropinocytosis, caveolae/lipid raft-mediated endocytosis, and clathrin-mediated endocytosis, respectively.¹² We incubated the cells with media containing wortmannin (10 μ M), filipin (1 μ M), or sucrose (0.45 M) for 1 hr, we then removed the media and added antisense and **DP** micelles samples for a further incubation of 24 hr. We then proceeded to quantify luciferase activity as described earlier. Micelle-forming **HE₁₂-Luc-ASO** luciferase knockdown

remained unchanged (60%) after filipin and sucrose treatment (Fig. SF11). However, wortmannin treatment lead to a significant increase in luciferase activity (70%). Taken together, our data suggests that DNA-polymers are likely trafficked to the cytoplasm through macropinocytosis. In previous studies, it was observed that PEI complexes were internalized via a clathrin-dependent route, a lipid-raft-dependent route, and macropinocytosis with the latter being more relevant with larger particle size.^{8, 40-43} Further investigation into the uptake mechanism of the PEI-micelle complexes is ongoing.

Conclusion

Highly efficient gene carriers such as linear PEI are not necessarily well suited for short nucleic acid delivery (antisense and siRNA) delivery. Indeed, while the B-PEI of 25 kDa and the linear PEI of 22 kDa are recognized as belonging to the most efficient plasmid DNA transfection agents, these polymers are poor transducers for the delivery of dsRNA duplexes.¹³ Additionally, L-PEI 25 kDa has been shown to be a poor delivery vehicle for exon-skipping oligonucleotides.^{44, 45} Only when L-PEI of this length is modified,^{12, 18, 46} is ASO delivery and knockdown enhanced.

Here we demonstrate that when antisense oligonucleotides targeting firefly luciferase are conjugated to micelle-forming polymers in a facile and reproducible method,²² we are able to significantly knockdown efficiency. Enhanced activity is dependent on micelle formation (**HE₁₂-Luc-ASO**). When the same ASO is conjugated to a polymer of similar length without the ability to associate to a micelle (**(HE-HEG)₆-Luc-ASO**), gene silencing activity is not observed. Furthermore, gene silencing activity is achieved even at an N:P=5 (< 1 µg/mL of PEI), with minimal cytotoxicity. While higher PEI concentrations (N:P=20) did increase antisense knockdown efficiency, a slight concomitant increase of cytotoxicity was observed. The cytotoxicity of HMW PEI is well studied^{37, 47, 48} and is especially detrimental at higher concentrations. Significant cytotoxicity and apoptotic cell death was demonstrated at concentrations of 10-20 µg/ml of HMW L-PEI and B-PEI (750 kDa and 25 kDa). Nonetheless, successful examples of *in*

in vivo applications for efficient carriers of siRNA have been demonstrated, specifically when PEI is integrated as a building block of nanoparticles.^{46, 49-51} Furthermore, we demonstrated that increased gene silencing is maintained over several days with similar resistance properties to spherical nucleic acid particles (SNAs).^{52, 53} SNAs have been demonstrated to be degradation-stable and efficient gene silencing vehicles.^{28, 54}

Using our approach, we are able to achieve significant transfection and knockdown with minimal cytotoxicity at much lower concentrations of L-PEI than previously needed (at N:P=5 and 10). Our approach is simple and efficient as it only requires readily available PEI at very low concentrations. The unique ability for low PEI requirement hinges on the intrinsic structure and monomer sequence of DNA polymers²² and their propensity to form highly ordered populations with relatively low nitrogen to phosphate content but high gene silencing potential. The polymers can be precisely controlled with respect to their sequence and length and are completely monodisperse, offering the possibility of additional tuning of transfection efficiency.

AUTHOR INFORMATION

Corresponding Author

Prof. Hanadi Sleiman

Department of Chemistry and Center for Self-Assembled Chemical Structures

McGill University

801 Sherbrooke St. W.

Montreal, QC H3A 0B8

Canada

Office: 417

Phone: (514) 398-2633

Fax: (514) 398-3797

e-mail: hanadi.sleiman@mcgill.ca

Author Contributions

All authors have given approval to the final version of the manuscript.

Funding Sources

NSERC, CIHR, FQRNT and QNRF.

ACKNOWLEDGMENT

We would like to thank Drs. Masad Damha and Glenn Deleavey for their expertise and for providing access the firefly luciferase HeLa cell line. We would like to also thank Ms. Henrietta Lacks and her family for providing access to the original lineage of HeLa cells.

ABBREVIATIONS

ASO: antisense oligonucleotide; PAGE: polyacrylamide gel electrophoresis; DLS: dynamic light scattering; RLU: relative fluorescence units; AFM: atomic force microscopy; TEM: transmission electron microscopy; L-PEI: linear poly(ethylenimine); B-PEI: branched poly(ethylenimine); HMW: high molecular weight; LMW: low molecular weight.

References

1. Machitani M, Yamaguchi T, Shimizu K, Sakurai F, Katayama K, Kawabata K and Mizuguchi H, *Pharmaceutics*, 2011, **3**, 338-353.
2. Pack DW, Hoffman AS, Pun S and Stayton PS, *Nat Rev Drug Discov*, 2005, **4**, 581-593.
3. Leong KW, Mao HQ, Truong-Le VL, Roy K, Walsh SM and August JT, *J. Control. Release*, 1998, **53**, 183-193.
4. Wang J, Zhang P-C, Lu H-F, Ma N, Wang S, Mao H-Q and Leong KW, *J. Control. Release*, 2002, **83**, 157-168.

5. Boussif O, Lezoualc'h F, Zanta MA, Mergny MD, Scherman D, Demeneix B and Behr JP, *Proceedings of the National Academy of Sciences*, 1995, **92**, 7297-7301.
6. Labat-Moleur F, Steffan AM, Brisson C, Perron H, Feugeas O, Furstemberger P, Oberling F, Brambilla E and Behr JP, *Gene Ther.*, 1996, **3**, 1010-1017.
7. Mislick KA and Baldeschwieler JD, *Proceedings of the National Academy of Sciences*, 1996, **93**, 12349-12354.
8. von Gersdorff K, Sanders NN, Vandenbroucke R, De Smedt SC, Wagner E and Ogris M, *Mol. Ther.*, 2006, **14**, 745-753.
9. Behr JP, *Chimia*, 1997, **51**, 34-36.
10. Pollard H, Toumaniantz G, Amos J-L, Avet-Loiseau H, Guihard G, Behr J-P and Escande D, *The Journal of Gene Medicine*, 2001, **3**, 153-164.
11. Itaka K, Harada A, Yamasaki Y, Nakamura K, Kawaguchi H and Kataoka K, *The Journal of Gene Medicine*, 2004, **6**, 76-84.
12. Xie J, Teng L, Yang Z, Zhou C, Liu Y, Yung BC and Lee RJ, *BioMed Research International*, 2013, **2013**, 710502.
13. Richards Grayson A, Doody A and Putnam D, *Pharm. Res.*, 2006, **23**, 1868-1876.
14. Neuberg P and Kichler A, *Adv. Genet.*, 2014, **88**, 263-288.
15. Thomas M, Ge Q, Lu JJ, Chen J and Klibanov A, *Pharm. Res.*, 2005, **22**, 373-380.
16. Tang GP, Yang Z and Zhou J, *J. Biomater. Sci. Polym. Ed.*, 2006, **17**, 461-480.
17. Gharwan H, Wightman L, Kircheis R, Wagner E and Zatloukal K, *Gene Ther.*, 0000, **10**, 810-817.
18. Teng L, Xie J, Teng L and Lee RJ, *Anticancer Res.*, 2012, **32**, 1267-1271.
19. Cortez MA, Godbey WT, Fang Y, Payne ME, Cafferty BJ, Kosakowska KA and Grayson SM, *J. Am. Chem. Soc.*, 2015, DOI: 10.1021/jacs.5b00980.
20. Patil Y and Panyam J, *Int. J. Pharm.*, 2009, **367**, 195-203.
21. Bolcato-Bellemin A-L, Bonnet M-E, Creusat G, Erbacher P and Behr J-P, *Proceedings of the National Academy of Sciences*, 2007, **104**, 16050-16055.
22. Edwardson TG, Carneiro KM, Serpell CJ and Sleiman HF, *Angew Chem Int Ed Engl*, 2014, **53**, 4567-4571.
23. Jensen SA, Day ES, Ko CH, Hurley LA, Luciano JP, Kouri FM, Merkel TJ, Luthi AJ, Patel PC, Cutler JI, Daniel WL, Scott AW, Rotz MW, Meade TJ, Giljohann DA, Mirkin CA and Stegh AH, *Science Translational Medicine*, 2013, **5**, 209ra152.
24. Walsh AS, Yin H, Erben CM, Wood MJA and Turberfield AJ, *ACS Nano*, 2011, **5**, 5427-5432.
25. Fakhoury JJ, McLaughlin CK, Edwardson TW, Conway JW and Sleiman HF, *Biomacromolecules*, 2014, **15**, 276-282.
26. Li J, Fan C, Pei H, Shi J and Huang Q, *Adv. Mater. (Weinheim, Ger.)*, 2013, **25**, 4386-4396.
27. Hamblin GD, Carneiro KMM, Fakhoury JF, Bujold KE and Sleiman HF, *J. Am. Chem. Soc.*, 2012, **134**, 5426-5426.
28. Banga RJ, Chernyak N, Narayan SP, Nguyen ST and Mirkin CA, *J. Am. Chem. Soc.*, 2014, **136**, 9866-9869.
29. Douglas SM, Bachelet I and Church GM, *Science*, 2012, **335**, 831-834.
30. Zhang Q, Jiang Q, Li N, Dai L, Liu Q, Song L, Wang J, Li Y, Tian J, Ding B and Du Y, *ACS Nano*, 2014, **8**, 6633-6643.
31. Liu H, Zhu Z, Kang H, Wu Y, Sefan K and Tan W, *Chemistry – A European Journal*, 2010, **16**, 3791-3797.
32. Alemdaroglu FE, Alemdaroglu NC, Langguth P and Herrmann A, *Macromolecular rapid communications*, 2008, **29**, 326-329.
33. Alemdaroglu FE, Alemdaroglu NC, Langguth P and Herrmann A, *Advanced Materials*, 2008, **20**, 899-902.

34. Rush AM, Nelles DA, Blum AP, Barnhill SA, Tatro ET, Yeo GW and Gianneschi NC, *Journal of the American Chemical Society*, 2014, **136**, 7615-7618.
35. Deleavey GF, Watts JK, Alain T, Robert F, Kalota A, Aishwarya V, Pelletier J, Gewirtz AM, Sonenberg N and Damha MJ, *Nucleic Acids Res.*, 2010, **38**, 4547-4557.
36. Zhao Q-Q, Chen J-L, Lv T-F, He C-X, Tang G-P, Liang W-Q, Tabata Y and Gao J-Q, *Biological and Pharmaceutical Bulletin*, 2009, **32**, 706-710.
37. Moghimi SM, Symonds P, Murray JC, Hunter AC, Debska G and Szewczyk A, *Mol. Ther.*, 2005, **11**, 990-995.
38. Kafil V and Omid Y, *BiolImpacts : BI*, 2011, **1**, 23-30.
39. Kim SH, Mok H, Jeong JH, Kim SW and Park TG, *Bioconjug. Chem.*, 2006, **17**, 241-244.
40. Zhang X-X, Allen PG and Grinstaff M, *Mol. Pharm.*, 2011, **8**, 10.1021/mp100366h.
41. Alhaddad A, Durieu C, Dantelle G, Le Cam E, Malvy C, Treussart F and Bertrand J-R, *PLoS One*, 2012, **7**, e52207.
42. Singh B, Maharjan S, Park TE, Jiang T, Kang SK, Choi YJ and Cho CS, *Macromol. Biosci.*, 2015, **15**, 622-635.
43. Liang S, Yang X-Z, Du X-J, Wang H-X, Li H-J, Liu W-W, Yao Y-D, Zhu Y-H, Ma Y-C, Wang J and Song E-W, *Adv. Funct. Mater.*, 2015, DOI: 10.1002/adfm.201501548, n/a-n/a.
44. Wang M, Wu B, Lu P, Tucker JD, Milazi S, Shah SN and Lu QL, *Gene Ther.*, 2014, **21**, 52-59.
45. Zaghoul EM, Viola JR, Zuber G, Smith CIE and Lundin KE, *Mol. Pharm.*, 2010, **7**, 652-663.
46. Dahlman JE, Barnes C, Khan OF, Thiriot A, Jhunjunwala S, Shaw TE, Xing Y, Sager HB, Sahay G, Speciner L, Bader A, Bogorad RL, Yin H, Racie T, Dong Y, Jiang S, Seedorf D, Dave A, Singh Sandhu K, Webber MJ, Novobrantseva T, Ruda VM, Lytton-JeanAbigail KR, Levins CG, Kalish B, Mudge DK, Perez M, Abezgauz L, Dutta P, Smith L, Charisse K, Kieran MW, Fitzgerald K, Nahrendorf M, Danino D, Tudor RM, von Andrian UH, Akinc A, Panigrahy D, Schroeder A, Kotliansky V, Langer R and Anderson DG, *Nat Nano*, 2014, **9**, 648-655.
47. Putnam D, Gentry CA, Pack DW and Langer R, *Proceedings of the National Academy of Sciences*, 2001, **98**, 1200-1205.
48. Breunig M, Hozsa C, Lungwitz U, Watanabe K, Umeda I, Kato H and Goepferich A, *J. Control. Release*, 2008, **130**, 57-63.
49. Francis SM, Taylor CA, Tang T, Liu Z, Zheng Q, Dondero R and Thompson JE, *Mol. Ther.*, 2014, **22**, 1643-1652.
50. Hanafi-Bojd MY, Jaafari MR, Ramezani N, Xue M, Amin M, Shahtahmassebi N and Malaekhe-Nikouei B, *Eur. J. Pharm. Biopharm.*, 2015, **89**, 248-258.
51. Chen Y, Gu H, Zhang DS, Li F, Liu T and Xia W, *Biomaterials*, 2014, **35**, 10058-10069.
52. Massich MD, Giljohann DA, Schmucker AL, Patel PC and Mirkin CA, *ACS Nano*, 2010, **4**, 5641-5646.
53. Seferos DS, Prigodich AE, Giljohann DA, Patel PC and Mirkin CA, *Nano Lett.*, 2009, **9**, 308-311.
54. Zheng D, Giljohann DA, Chen DL, Massich MD, Wang X-Q, Iordanov H, Mirkin CA and Paller AS, *Proceedings of the National Academy of Sciences*, 2012, **109**, 11975-11980.

SYNOPSIS

